CHEMISTRY
A EUROPEAN JOURNAL

DOI: 10.1002/chem.200801030

Predicting Reactivity and Stereoselectivity in the Nazarov Reaction: A Combined Computational and Experimental Study

Andrea Cavalli,*[a] Alessandro Pacetti,[a] Maurizio Recanatini,[a] Cristina Prandi,[b] Dina Scarpi,[c] and Ernesto G. Occhiato*[c]

Abstract: The Nazarov reaction of pentadienyl cations generated by protonation of either dienones or alkoxytrienes has been examined in detail both experimentally and by DFT calculations. In particular, calculations at the B3LYP/6-311G** level of theory accurately predicted, and accounted for, the outcome of the Brønsted acid catalyzed electrocyclization of 4π-electron systems in which one of the double bonds involved in the process was embedded in N- and S-heterocyclic rings. Calculations showed that both heteroatoms are capable of accelerating the ring closure by stabilizing the partial positive charge which develops at C-6 (C-2) in the transition state, with S-heterocyclic derivatives being more reactive than the corresponding N-containing compounds. In general, pentadienyl cations generated by protonation of alkoxytrienes were expected to react faster than those obtained by protonation of the corresponding dienones, as the latter were stabilized by a hydrogen bond. The presence of a substituent on the heterocyclic ring significantly affects the stereoselectivity (torquoselectivity) only in the case of the N-heterocyclic derivatives, in which a 2-alkyl group is axially oriented, providing the *cis*-2,5-disubstituted isomer only. Instead, with substituted S-heterocyclic compounds, the anticipated torquoselectivity was very low and, in fact, a 3:1 diastereomeric mixture between the *trans* and *cis* products was experimentally found after ring closure. For this study, the synthesis of the appropriate N- and S-containing dienones and alkoxytrienes was realized to evaluate the predictivity power of the DFT computations, which was very good in all of the cases examined, both in terms of reactivity and stereoselectivity. The consistency observed between computational and experimental results, therefore, shows the usefulness of DFT calculations at the B3LYP/6-311G** level of theory as a robust instrument for the prediction of reactivity and stereoselectivity in the Nazarov electrocyclic reaction.

Keywords: density functional calculations · electrocyclic reactions · Nazarov reaction · reaction mechanisms · torquoselectivity

Introduction

Electrocyclic reactions, especially 1,3-cyclohexadiene formation, cyclobutene ring opening, and Nazarov and related cationic cyclizations are of great importance in organic chemistry as synthetic tools for the construction of the molecular skeleton of complex natural and biologically active compounds.[1–3]

Reactivity and stereoselectivity are relevant issues in these processes. Electrocyclization reactions can be in fact energetically demanding processes, often requiring conditions incompatible to sensitive substrates, so that a proper choice of substituent on the π system, or structural modifications of the latter, are often necessary to attain synthetically favorable reaction conditions. The stereoselectivity in the ring opening/closure, referred to as "torquoselectivity", is the preference for one of the two orbital symmetry allowed modes by which every electrocyclic reaction can occur.[4]

[a] Dr. A. Cavalli, A. Pacetti, Prof. M. Recanatini
Dipartimento di Scienze Farmaceutiche
Alma Mater Studiorum—Università di Bologna
Via Belmeloro 6, 40126 Bologna (Italy)
Fax: (+39) 051-2099734
E-mail: andrea.cavalli@unibo.it

[b] Prof. C. Prandi
Dipartimento di Chimica Generale e Chimica Organica
Università di Torino, Corso Massimo D'Azeglio, 48
10125 Torino (Italy)

[c] Dr. D. Scarpi, Dr. E. G. Occhiato
Dipartimento di Chimica Organica "U. Schiff"
Università di Firenze, Via della Lastruccia 13
I-50019 Sesto Fiorentino (Italy)
Fax: (+39) 055-457-3531
E-mail: ernesto.occhiato@unifi.it

Supporting information for this article is available on the WWW under http://dx.doi.org/10.1002/chem.200801030.

Again, suitable substituents can strongly influence the torquoselectivity, as in the well-studied cases of the "inward" or "outward" conrotatory thermal ring opening of cyclobutenes,[5] and the conrotatory "clockwise" or "counterclockwise" thermal Nazarov cyclization of 1,4-pentadien-3-ones.[6–10] Thus, an in-depth understanding of how steric and electronic features of the substituents affect the reaction outcome is invaluable for the synthetic design. To this end, computational methods based on first principles can be exploited for the theoretical prediction of both reactivity and stereoselectivity in electrocyclic processes.[11]

Among the electrocyclic reactions, the Nazarov reaction has recently emerged as one of the most powerful processes for constructing five-membered carbocyclic systems, after having found applications in the synthesis of several natural products.[12] The Nazarov reaction of N- and O-heterocyclic divinyl ketones and their synthetic equivalents depicted in Figure 1a has been, in particular, the subject of several recent studies.[13–18] The cyclization forms cyclopenta-fused

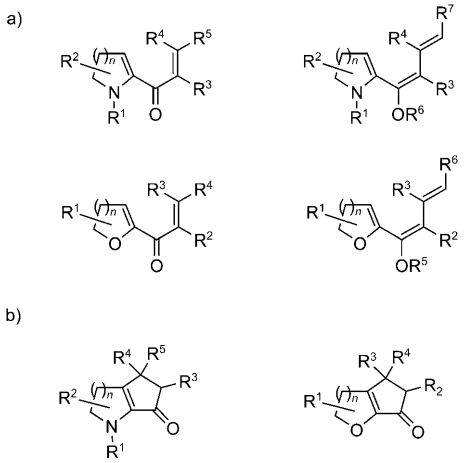

Figure 1. a) Substrates for and b) products of the Nazarov reaction involving heterocyclic systems.

heterocyclic compounds (Figure 1b), the interest of which arises from their presence in several natural and biologically active compounds.[12,19]

The presence of the heteroatom has a noteworthy influence on the reactivity of these systems, as it makes the ring closure of the corresponding pentadienyl cations possible even in the presence of catalytic amounts of Brønsted[15c–e,17] or Lewis acids[14,15a–b,16] at room temperature. Conversely, the corresponding carbocyclic substrates do not generally react unless more drastic conditions are used.[15d] Even more striking is the stereoselectivity in the ring closure of these systems. For example, it has been observed that whilst the 2,5-*trans* disubstituted compounds **5** (Scheme 1) are the major diastereomers obtained in the electrocyclization of the O-containing substrates **2**,[17] by contrast N-heterocyclic dienone equivalents **7** (Scheme 2) give exclusively the 2,5-*cis* disubstituted products **10**.[15d] The same results have recently been obtained also in the Lewis acid catalyzed Nazarov reaction of divinyl ketones, such as **1** (Scheme 1).[15a]

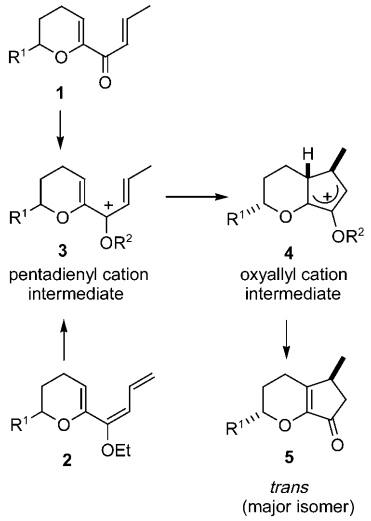

Scheme 1. Torquoselectivity in the Nazarov reaction of O-heterocyclic dienones and alkoxytrienes.

Recently, various authors have demonstrated that either ab initio or DFT calculations are well suited to provide an in-depth understanding of the Nazarov reaction mechanism, the nature of which could not be straightforwardly interpreted.[6,8–10,18,20] In particular, in our previous study, we demonstrated that DFT calculations at the B3LYP/6-311G** level of theory were well suited to account for the electrocyclization outcome of the 4π-electron system of heterocyclic 2,3-alkoxypentadienyl cations **3** (Scheme 1),[17] both in terms of reactivity and torquoselectivity.[18] This study allowed us to assess the role of the 2-alkoxy substituent in increasing the reaction rate,[17] as was recently further confirmed by Frontier,[14a] and to establish that the stereoselectivity in the cyclopentannulation was mainly dictated by stereoelectronic effects. The agreement of the theoretical calculations with the experimental results encouraged us to apply the same calculation protocol both to predict, and to account for, the reactivity and torquoselectivity in the Brønsted acid catalyzed electrocyclization of the analogous N- and S-substituted heterocyclic systems that have never been comprehensively dealt with before (Scheme 2). In this study, we report on a comparison between the predictive results of a detailed theoretical study on the rate-determining step's energy profile of the Nazarov reaction involving N- and S-substituted heterocyclic systems and the experimental reaction outcome for the corresponding series of substrates. In the light of the consistency observed between computational and experimental results, the usefulness of DFT calculations as a robust instrument to anticipate reactivity and stereoselectivity in such electrocyclic reactions is demonstrated.

Results and Discussion

The equations studied for evaluating the role of the heteroatom (N, S) on the reactivity are depicted below [Eqs. (1–

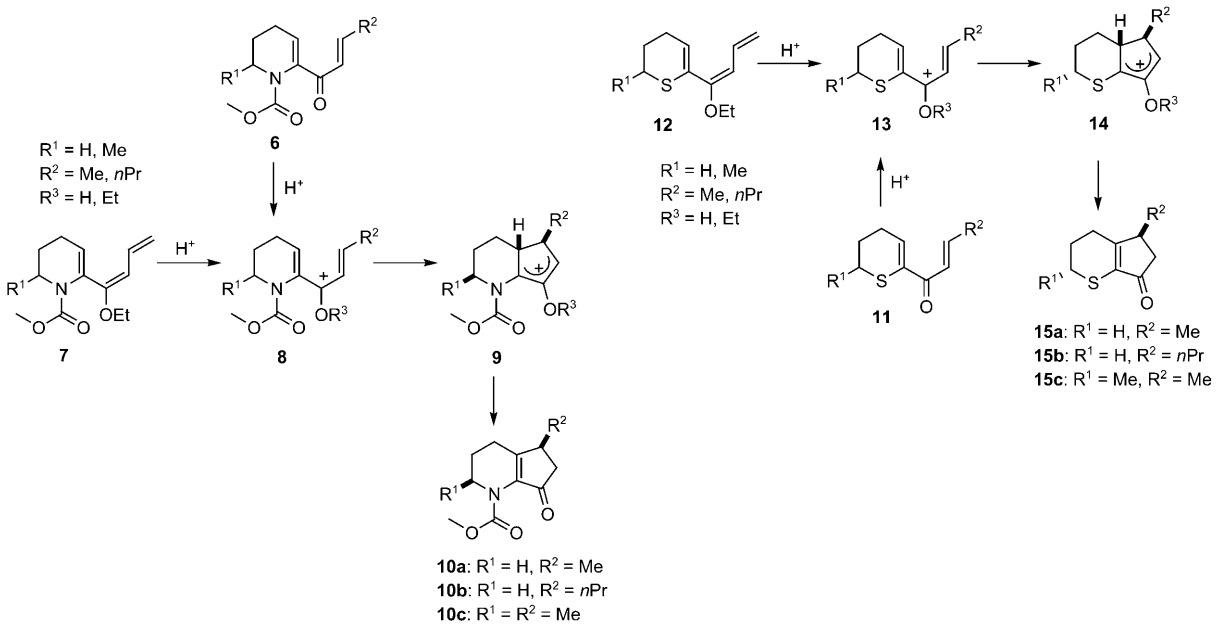

Scheme 2. The Nazarov reaction of N- and S-heterocyclic dienones and alkoxytrienes.

4)]. The reaction of a 2-methyl-substituted N-heterocyclic pentadienyl cation is depicted in Equation (5) and represents our case-study to find a rational for the complete 2,5-*cis* stereoselectivity observed in the ring closure of N-containing derivatives.[15d] *N*-CO_2Me was chosen as the protecting group instead of *N*-Cbz (Cbz: carbobenzyloxy) or *N*-Ts (Ts: tosyl), generally used in our previous synthetic studies, to reduce the conformational complexity. Finally, the reaction of a 2-methyl-substituted S-heterocyclic derivative [Eq. (6)] represents the case studied here for predicting the torquoselectivity in the Nazarov reaction of S-containing systems.

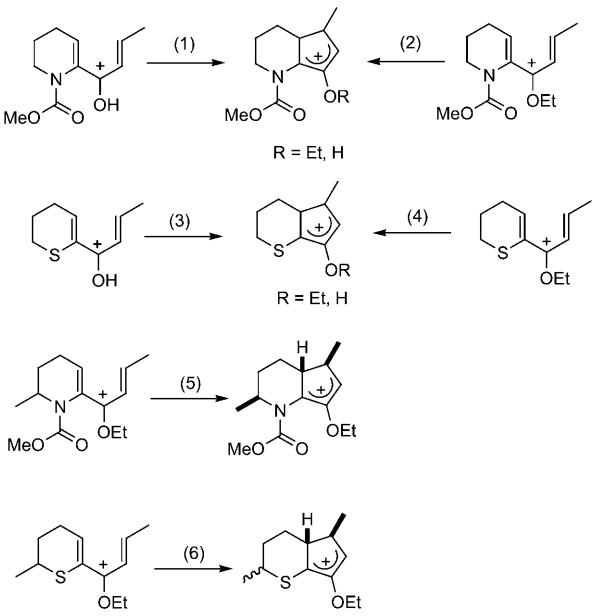

Prediction of the reactivity: The Nazarov reaction is a conrotatory electrocyclization process. When one of the double bonds involved in the electrocyclization is embedded in a (hetero)cyclic structure, the formation of the new bond can take place either along the axial (Scheme 3, path a) or equatorial direction (path b), depending on the conformation of the ring. We have already shown that path a is preferred with O derivatives (X=O) as it allows for the maximum orbital overlap in the forming C5–C3′ (C4a–C5) bond.[18] In Figures 2–4, the DFT-computed energy surfaces for paths a and b of Equations (1–4) are reported. In Tables 1–4, the relative electronic and free energies and the geometrical parameters of all stationary points are reported and, in Figure 5, a representation of the atom numbering used in the text is shown.

In Figure 2, the energy profiles of Equation (1) are reported, which refers to the electrocyclization of the pentadienyl cation **8** (R^1=H, R^2=Me, R^3=H) obtained after protonation of the carbonyl group in the corresponding N-heterocyclic divinyl ketone **6** ("classic" Nazarov reaction). The simplest substitution on the vinyl moiety (R^3=Me) was chosen to reduce the number of conformers.

In all of the *N*-CO_2Me-protected compounds, the presence of the protecting group doubled the number of initial conformations of the pentadienyl cationic intermediates, as found by Monte Carlo conformational searches. Figure 2a and b refer to the initial conformations in which the C=O of *N*-CO_2Me points toward the hydroxyl group, forming a hydrogen bond in the global minimum conformer **I**; Figure 2c and d refer to the initial conformations in which the MeO group is roughly oriented towards the hydroxyl group.

By the analysis of the energy profiles, it clearly appears that the reaction is exothermic, similar to the Nazarov reaction of the O-substituted analogues[18] and other substra-

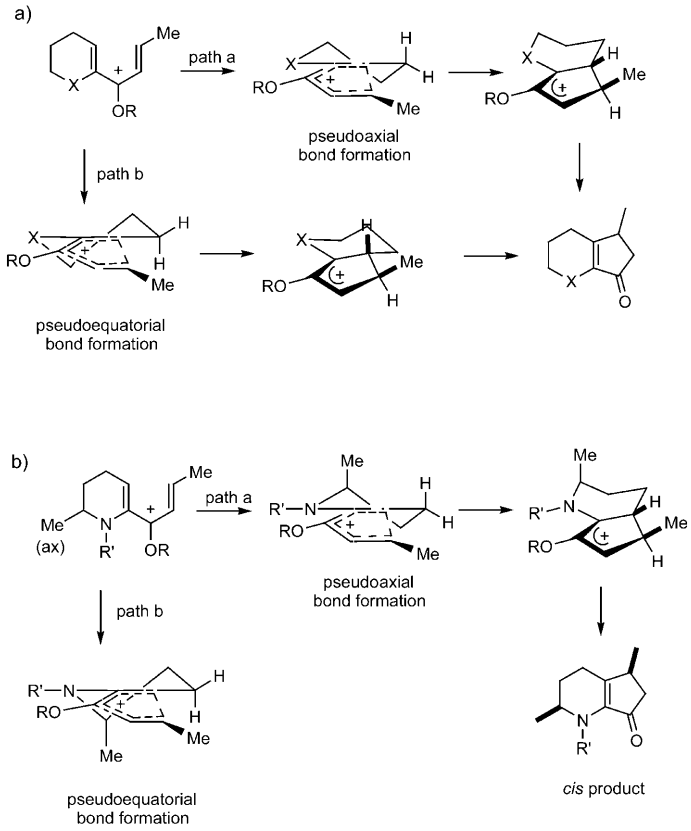

Scheme 3. The different conrotation modes of the Nazarov reaction involving (hetero)cyclic structures.

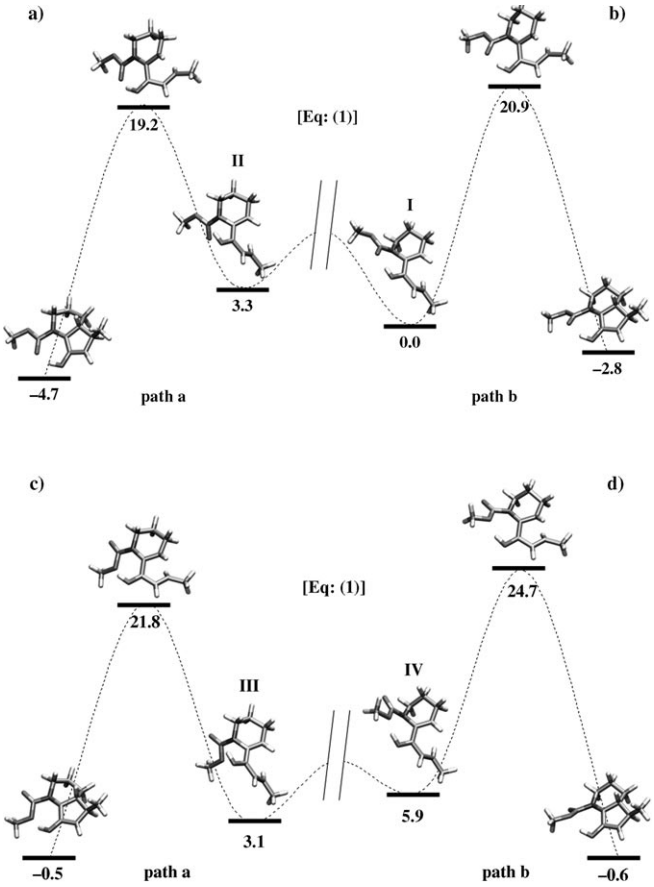

Figure 2. The free-energy profiles (in kcal mol^{-1}) for Equation (1). Four conformers (a–d) of the reactant were taken into account to explore all possible energy profiles. Paths a and b refer to Scheme 3.

Table 1. Energies and geometrical parameters for Equation (1).[a]

Equation		ΔE_{elec}	$\Delta(E_{elec}+$ ZPVE)	$\Delta G_{gas\ phase}$	ΔG_{total}	C5–C3′ [Å]
1 (Figure 2a)	react.	5.5	6.5	6.1	3.3	3.24
	TS	20.8$^{\neq}$	21.2$^{\neq}$	21.4$^{\neq}$	19.2$^{\neq}$	2.19
	prod.	−5.1	−2.5	−2.9	−4.7	1.54
1 (Figure 2b)	react.	0	0	0	0	3.15
	TS	22.2$^{\neq}$	23.0$^{\neq}$	23.3$^{\neq}$	20.9$^{\neq}$	2.16
	prod.	−5.0	−2.4	−1.7	−2.8	1.54
1 (Figure 2c)	react.	7.6	8.5	8.0	3.1	3.22
	TS	25.3$^{\neq}$	25.7$^{\neq}$	26.0$^{\neq}$	21.8$^{\neq}$	2.21
	prod.	−0.3	2.1	2.4	−0.5	1.54
1 (Figure 2d)	react.	8.7	9.5	9.3	5.9	3.13
	TS	28.2$^{\neq}$	28.8$^{\neq}$	29.3$^{\neq}$	24.7$^{\neq}$	2.16
	prod.	−0.6	1.8	2.4	−0.6	1.55

[a] react.: pentadienyl cation; TS: transition state; prod.: oxyallyl cation. Energy values are in kcal mol^{-1}

tes.[9,20b] The formation of the new bond along the axial direction (path a) disrupts (in **II**) the stabilizing hydrogen bond in **I** (distance C=O···HO = 1.34 in **I**, 2.87 Å in **II**), which is only weakly restored in the transition state (distance C=O···H = 1.63 Å) (Figure 2a). The activation energy ($\Delta G^{\neq}$) of this process (19.2 kcal mol^{-1}) is almost 2 kcal mol^{-1} lower than that of path b, the transition state (TS) of which maintains a weaker hydrogen bond (distance C=O···HO = 1.56 Å) than in **I**. The chemical processes reported in Figure 2c and d are both highly energetic (21.8 and 24.7 kcal mol^{-1} for path a and b, respectively). As a consequence, with the lowest activation energy at about 19 kcal mol^{-1}, we may anticipate that a compound such as **6** ($R^1 = R^2 = H$) will not react at room temperature after generation of the corresponding cationic intermediate **8** in the presence of a proton (H^+) source.[21]

When the ethoxy group replaces the OH in the pentadienyl cation ([Eq. (2)] and Figure 3a–d), generally lower TS energies were obtained (with the reaction being still exothermic). The lowest activation energy is still associated to a bond formation along the axial direction (16.1 kcal mol^{-1}, Figure 3a), although the differences found among the four profiles were less important than in the case of Equation (1). In analogy to what was observed in our previous work on similar O-containing derivatives **2**,[18] the lower activation energies associated with the presence of the ethoxy group could be accounted for by the lack, in the starting pentadienyl cationic intermediates **V**–**VIII**, of the hydrogen bond that instead stabilizes intermediate **I** (Figure 2b). As the lowest activation energy is 16.1 kcal mol^{-1} for the electrocyclization of **7** ($R^1 = H$), this process is more favored than that of divinyl ketone **6** ($R^1 = H$, $R^2 = Me$; $\Delta G^{\neq} = 19.2$ kcal mol^{-1}) and we expect that the former reaction could occur at room temperature, although quite slowly.

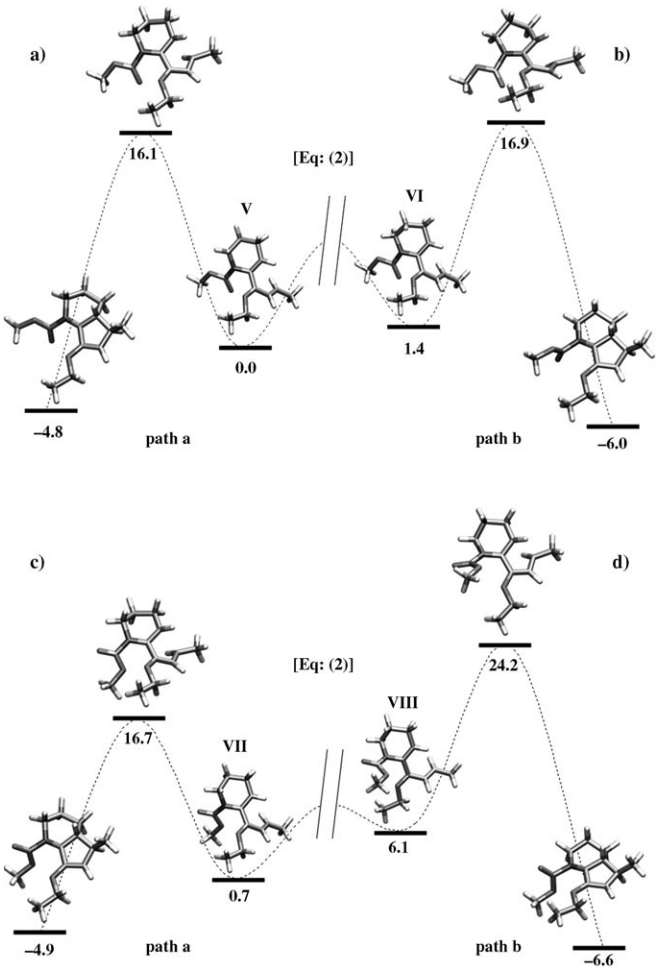

Figure 3. The free-energy profiles (in kcal mol^{-1}) for Equation (2). Four conformers (a–d) of the reactant were taken into account to explore all possible energy profiles. Paths a and b refer to Scheme 3.

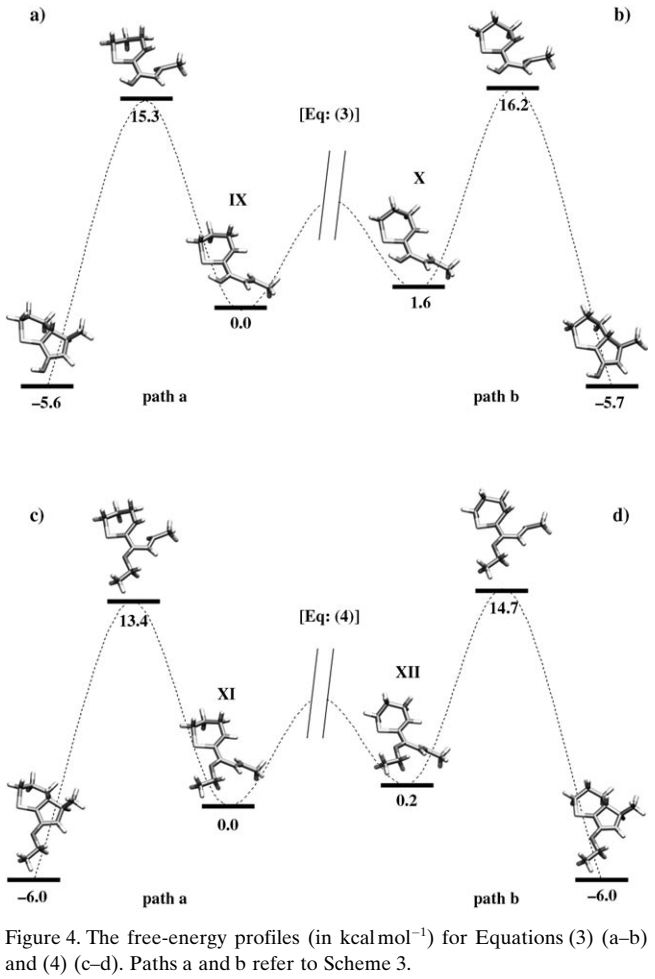

Figure 4. The free-energy profiles (in kcal mol^{-1}) for Equations (3) (a–b) and (4) (c–d). Paths a and b refer to Scheme 3.

Finally, concerning the S-containing derivatives, Equations (3) and (4), the cyclization of global minimum conformer **IX** ([Eq. (3)], Figure 4a) has a barrier of 15.3 kcal mol^{-1} if the new bond forms along the axial direction (path a), slightly lower than the barrier associated with path b (Figure 4b). When the ethoxy replaces the OH group in the pentadienyl cation [Eq. (4)], consistently to the N and O cases, the activation energies were lowered to a value of around 13–15 kcal mol^{-1} (Figure 4c–d), the formation of the bond along the axial direction (path a) being always the favored one. Here too, we can hypothesize that such an effect is due to the lack of a stabilizing OH···S interaction in the starting pentadienyl cationic intermediates (distance OH···S = 2.34 in **IX**, 2.77 Å in the TSs of Equation (3).[22] In both cases, we may expect that the reaction can occur at room temperature, although again the cyclization of the ethoxytriene derivative should be faster.

In the cases so far analyzed, it is worth noticing that the newly C5−C3′-forming bond in the TS of the preferred cyclization modes (paths a in Figures 1–4) is always longer (d = 2.17–2.20 Å) than that previously found by calculations at the HF/6-31G* level of theory for open-chain substrates (d = 2.09 Å)[6c] pointing to an early TS in the Nazarov reaction in-

Table 2. Energies and geometrical parameters for Equation (2). Energy values are in kcal mol^{-1}.[a]

Equation		ΔE_{elec}	$\Delta(E_{elec}$+ZPVE)	$\Delta G_{gas\text{-}phase}$	ΔG_{total}	C5−C3′ [Å]	C2-N1-C6 [°]
2 (Figure 3a)	react.	0	0	0	0	3.21	118.0
	TS	16.0^{+}	15.8^{+}	16.8^{+}	16.1^{+}	2.20	117.2
	prod.	−6.0	−4.7	−4.1	−4.8	1.55	117.0
2 (Figure 3b)	react.	1.3	1.3	1.1	1.4	3.23	120.2
	TS	16.5^{+}	16.3^{+}	17.5^{+}	16.9^{+}	2.23	121.3
	prod.	−7.0	−5.4	−5.1	−6.0	1.55	123.3
2 (Figure 3c)	react.	4.1	4.1	4.2	0.7	3.17	116.4
	TS	18.8^{+}	18.5^{+}	19.6^{+}	16.7^{+}	2.22	117.2
	prod.	−5.6	−4.0	−3.7	−4.9	1.55	117.3
2 (Figure 3d)	react.	11.0	10.8	10.6	6.1	3.15	114.1
	TS	28.5^{+}	27.9^{+}	28.5^{+}	24.2^{+}	2.21	117.6
	prod.	−7.4	−5.9	−5.7	−6.6	1.55	123.1

[a] react.: pentadienyl cation; TS: transition state; prod.: oxyallyl cation.

Table 3. Further relevant geometrical parameters for Equation (2).[a]

Equation		O2″–O5′ [Å] O3″–O5′ [Å]	C6-N1-C1″-O2″ [°] C6-N1-C1″-O3″ [°]	N1-C6 -C1′-O5′ [°]
2 (Figure 3a)	react.	2.78	5.1	−42.3
	TS	2.71	−10.8	−37.0
	prod.	2.78	−46.5	−8.2
2 (Figure 3b)	react.	2.74	5.1	−47.4
	TS	2.72	−11.3	−36.9
	prod.	2.97	−80.3	−13.9
2 (Figure 3c)	react.	2.86	4.5	−32.3
	TS	2.77	−14.2	−34.1
	prod.	2.80	−58.6	−7.3
2 (Figure 3d)	react.	2.73	−6.8	−8.7
	TS	2.65	22.5	−24.1
	prod.	2.97	86.4	−11.4

[a] react.: pentadienyl cation; TS: transition state; prod.: oxyallyl cation.

Table 4. Energies and geometrical parameters for Equations (3) and (4). Energy values are in kcal mol^{-1}.[a]

Equation		ΔE_{elec}	$\Delta(E_{elec}+$ ZPVE)	$\Delta G_{gas\ phase}$	ΔG_{total}	C5–C3′ [Å]
3 (Figure 4a)	react.	0	0	0	0	3.19
	TS	16.8^{+}	16.3^{+}	17.3^{+}	15.3^{+}	2.17
	prod.	−3.0	−4.7	−4.0	−5.6	1.56
3 (Figure 4b)	react.	1.8	1.8	1.4	1.6	3.19
	TS	17.3^{+}	17.0^{+}	17.8^{+}	16.2^{+}	2.20
	prod.	−3.9	−5.5	−4.4	−5.7	1.56
4 (Figure 4c)	react.	0	0	0	0	3.09
	TS	13.1^{+}	12.8^{+}	13.8^{+}	13.4^{+}	2.19
	prod.	−8.7	−7.1	−6.2	−6.0	1.55
4 (Figure 4d)	react.	0.3	0.3	0.3	0.2	3.14
	TS	14.1^{+}	14.0^{+}	14.9^{+}	14.7^{+}	2.23
	prod.	−9.5	−7.8	−6.3	−6.0	1.56

[a] react.: pentadienyl cation; TS: transition state; prod.: oxyallyl cation.

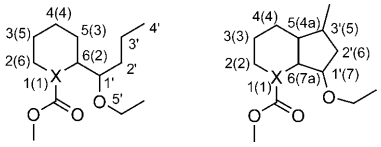

Figure 5. Atom numbering used in the text and tables. The IUPAC numbering is reported in brackets.

volving N- and S-heterocyclic systems. This is not dissimilar from what was found out in: 1) the computations on the same reaction with the corresponding O-heterocyclic substrates[18] and 2) previously reported quantum mechanical calculations on the Nazarov reaction of α-alkoxy-substituted hydroxypentadienyl cations.[9] Fitting with the early nature of the TSs, all reactions so far considered have been calculated to be exothermic.

Interestingly, while the activation energies associated with the cyclization of the ethoxy-substituted S derivative in Equation (4) (Figure 4c) is almost identical to that we have previously calculated for the corresponding O derivative (13.4 vs. 13.7 kcal mol^{-1}),[18] in the case of the N-heterocyclic derivatives ([Eq. (2)], Figure 3a), the $\Delta G^{\neq}$ value is appreciably higher (16.1 kcal mol^{-1}). By analysis of the geometrical parameters of intermediate **V** and the **TS** in Figure 3a (Tables 2 and 3) it comes out that in intermediate **V** there is a full conjugation between the N atom (which conserves its sp^2 hybridization all along the profile, see C2-N1-C6 bond angles) and the CO_2Me-protecting group (dihedral angle C6-N-C=O=5.1°). Moreover, the carbonyl and the ethoxy groups are far apart (d=2.78 Å), so reducing possible repulsive interactions. However, during the bond formation (in TS) a rotation around the C6–C1′ bond has to take place and the double bond starts to form between C6 and C1′. The consequence of this is the mounting of an A$^{(1,3)}$ allylic strain with the N-protecting group, which rotates around the N–CO bond (dihedral angle C6-N-C=O=−10.8°) to relieve the repulsive interaction between the two O atoms (the distance of which is now 2.71 Å). The consequential loss of conjugation between the N atom and the CO group, and the smaller C=O···OEt distance in TS than in intermediate **V**, can explain the higher activation energy if compared to the corresponding cases in which an X-protecting group is lacking (S and O derivatives). In the bicyclic intermediate, the conjugation is then completely broken to relieve the repulsive interaction between the two O atoms as suggested by the dihedral angle value of −46.5°.

As the N atom maintains its sp^2 hybridization all along the profile of Equation (2) (C2-N-C6 bond angle values from 118.0 to 117.0°), we may reckon that the N atom conjugates with the C6 atom on which a positive charge develops in the TS. Stabilization of the positive charge by the N atom (as in the case of the O derivatives) can be reasonably assumed to be the cause of the much lower activation energy associated with Equation (2) (16.1 kcal mol^{-1}) than that of the corresponding carbacyclic system (18.9 kcal mol^{-1}),[18] and this could be true also for the case of the S derivative in Equation (4). To demonstrate such an effect, we calculated the atomic partial charges on the N atom of the positively charged intermediate **V** and the TS of Equation (2) (Figure 3a) by the RESP-fitting procedure (see Methods). It turned out that the heterocyclic N atom had a partial atomic charge of −0.50 in **V**, whereas this was −0.34 in the TS. The decrease of the partial negative charge on the N atom found in the TS demonstrates that the heteroatom effectively conjugates with the p orbitals of the TS, thus providing a greater stabilization effect on the positive charge of the TS than on that of the starting intermediate. The stabilization of the positive charge that develops at C6 also occurs in the TS of Equation (4) (Figure 4c) relative to the Nazarov reaction of the S-heterocyclic pentadienyl cation. In this case, the heterocyclic S atom had a partial atomic charge of −0.08 in the starting intermediate **XI**, whereas this was +0.03 in the TS. Furthermore, we also carried out single-point calculations by neutralizing the positive charge on the system through the addition of one electron to both the starting intermediate **V** and the TS of Equation (2) (Figure 3a) (see Methods). It turned out that the energy barrier of the electrocyclization reaction was of 29.8 kcal mol^{-1} (vs. 16.1 kcal mol^{-1}), this increase being mainly due to a much greater stabilization of the starting intermediate **V** (Δele-

ctronic energy = −84.3 kcal mol^{-1}) with respect to the TS (Δelectronic energy = −70.6 kcal mol^{-1}). Analogously for the S derivatives (Equation (4), Figure 4c), the energy barrier of the electrocyclization reaction was 28.1 kcal mol^{-1} (vs. 13.4 kcal mol^{-1}) after addition of one electron because of a much greater stabilization of the starting intermediate **XI** (Δelectronic energy = −183.3 kcal mol^{-1}) with respect to the TS (Δelectronic energy = −168.5 kcal mol^{-1}).

Experimental assessment of the theoretical predictions: We have previously seen that the $\Delta G^{\neq}$ values, obtained by our calculations, lower than 14 kcal mol^{-1}, corresponded to fast reactions at room temperature. Conversely, when $\Delta G^{\neq}$ values were more than 18 kcal mol^{-1}, the corresponding reactions did not occur at room temperature.[18] Values ranging from around 15–16 kcal mol^{-1} corresponded to a slow reaction requiring at least 24 h to be completed under our conditions. On these bases, the above theoretical predictions were tested experimentally by preparing, as depicted in Scheme 4,

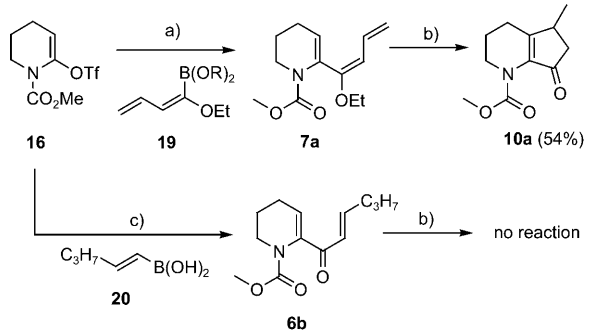

Scheme 4. Synthesis of N-heterocyclic dienones and alkoxytrienes: a) 5% $[PdCl_2(Ph_3P)_2]$, 2 M K_2CO_3 (aq), THF, 0.5 h, 25 °C; b) Amberlyst 15, CH_2Cl_2, 18 h, 25 °C; c) 5% of $Pd(OAc)_2$, 10% of Ph_3P, CO (1 atm), CsF, THF, 25 °C.

compound **7a** according to a methodology previously reported for similar compounds[15c–e] and subjecting it to hydrolysis in the presence of Amberlyst 15 in dichloromethane at room temperature. When monitoring the reaction by TLC, we found it to be quite slow and it was completed only after 18 h at room temperature, although accompanied by partial decomposition of the starting material, providing **10a** in 54% yield after chromatography.

By starting from the same triflate **16**, we prepared dienone **6b** by the carbonylative Suzuki–Miyaura coupling we have recently described[15b,23] (**6b** possesses a *n*-propyl moiety instead of the methyl group on the external double bond).[24a,b] This compound was treated with Amberlyst 15 under the usual conditions but, after 24 h, we recovered it completely unreacted (and without traces of decomposition byproducts).[25] Both results are perfectly in accordance with the $\Delta G^{\neq}$ values of 16.1 and 18.9 kcal mol^{-1} calculated for the two cyclization reactions, respectively.

The prediction of the reactivity was equally accurate when a sulfur atom was put in the place of the nitrogen in our ethoxytrienes and dienones. For the S derivatives, we should expect faster reactions than with N derivatives, taking into account the calculated $\Delta G^{\neq}$ values. As reported in Scheme 5, we prepared ethoxytriene **12a** and dienone **11**

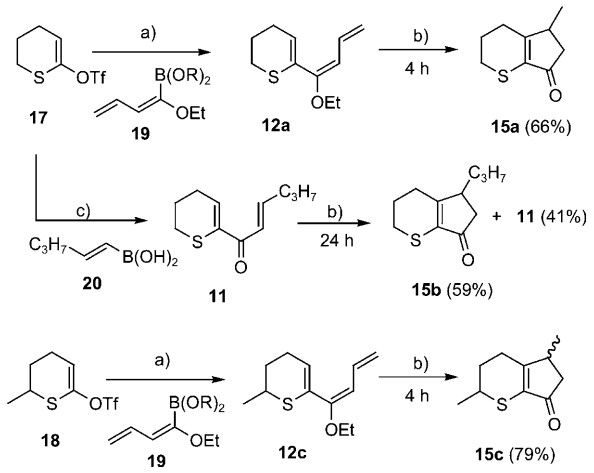

Scheme 5. Synthesis of S-heterocyclic dienones and alkoxytrienes: a) 5% $[PdCl_2(Ph_3P)_2]$, 2 M K_2CO_3 (aq), THF, 0.5 h, 25 °C; b) Amberlyst 15, CH_2Cl_2, 4–24 h, 25 °C; c) 5% of $Pd(OAc)_2$, 10% of Ph_3P, CO (1 atm), CsOAc, THF, 25 °C.

according to the usual methodologies,[15,24] and subjected them to treatment with Amberlyst 15 in CH_2Cl_2. After 4 h, the conversion of **12a** to **15a** was complete. Based on the $\Delta G^{\neq}$ values (15.3 vs. 13.4 kcal mol^{-1}), we could expect a slower cyclization of **11** to **15b** and perfectly in accordance we found that the conversion to **15b** was only about 59% after 24 h.

Stereoselectivity in the ring closure (torquoselectivity): A synthetically important aspect of the Nazarov reaction is the torquoselectivity of the electrocyclization process when one or more substituents are present on the cycle, which embeds the double bond.[12e,g] A surprisingly high remote stereocontrol was reported in the ring closure of dihydropyranyl derivative **3** (Scheme 1), which formed the 2,5-*trans*-disubstituted Nazarov product **5** as the major isomer.[17] DFT calculations showed that the pseudoaxial bond formation is kinetically preferred as it allows the maximum orbital overlap in a TS in which the R^1 substituent is equatorially oriented,[18] thus leading to the 2,5-*trans* compound.

The results obtained by us in the electrocyclization of the correspondingly substituted N derivative **7** (R^1 = Me), which leads to the exclusive formation of the 2,5-*cis*-disubstituted Nazarov product **10c** (Scheme 2) could instead be explained by taking into account that the 2-methyl group on the tetrahydropyridine ring should be axially oriented to remove the $A^{(1,3)}$ strain with the N-protecting group.[26] To find support for this hypothesis, we carried out a DFT study on the cyclization reported in Equation (5). The energy profiles are reported in Figure 6, and the geometrical parameters in Table 5. A Monte Carlo conformational search carried out

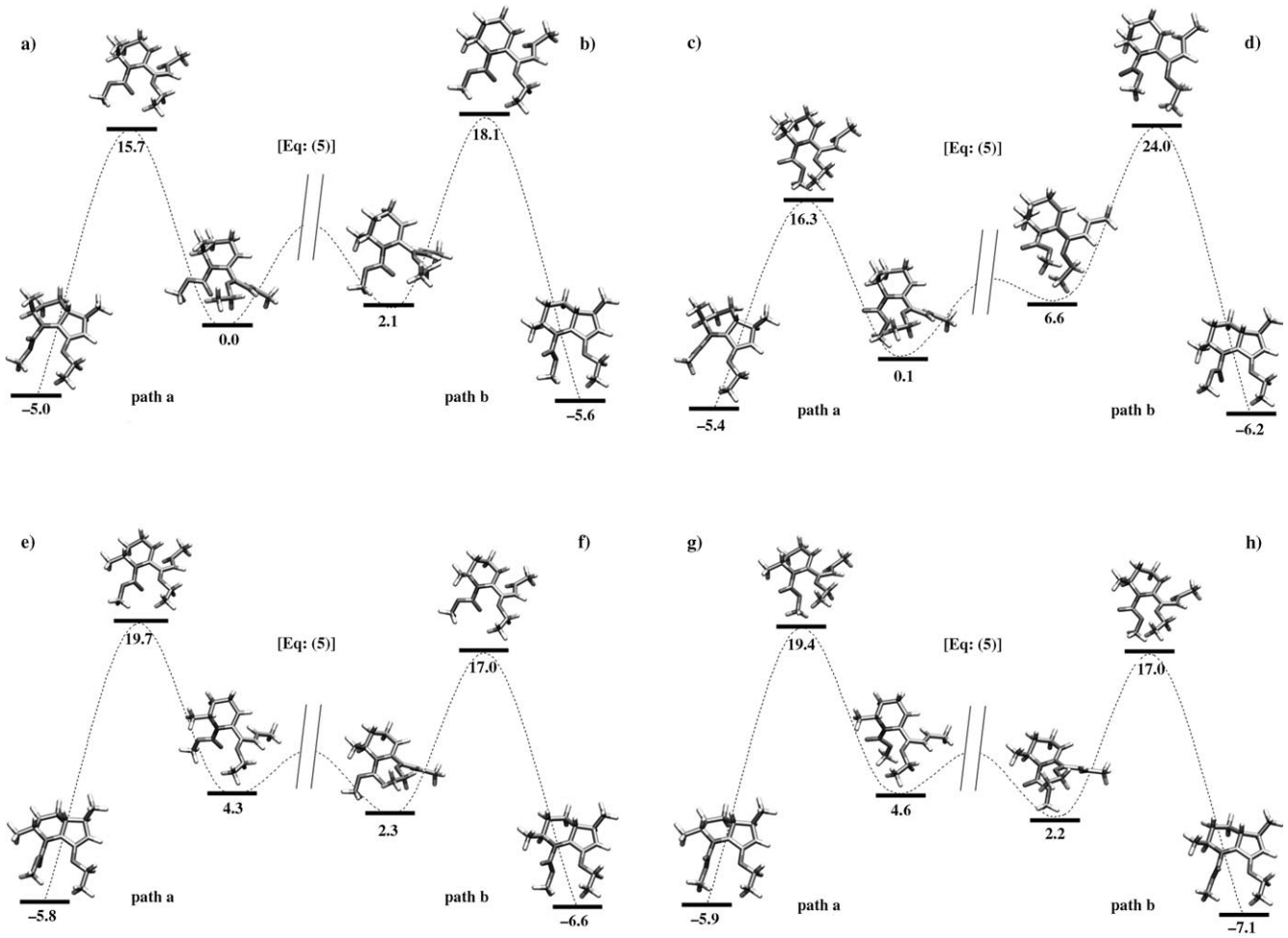

Figure 6. The free-energy profiles (in kcal mol^{-1}) for Equation (5). Eight conformers (four axial (a–d) and four equatorial (e–h)) of the reactant were taken into account to explore all possible energy profiles. Paths a and b refer to Scheme 3.

Table 5. Energies and geometrical parameters for Equation (5). Energy values are in kcal mol^{-1}.[a]

Equation		ΔE_{elec}	$\Delta(E_{elec}+$ ZPVE)	$\Delta G_{gas\ phase}$	ΔG_{total}	C5–C3′ [Å]
5 (Figure 6a)	react.	0	0	0	0	3.22
	TS	15.9$^{\neq}$	15.7$^{\neq}$	16.6$^{\neq}$	15.7$^{\neq}$	2.21
	prod.	−6.0	−4.4	−3.9	−5.0	1.56
5 (Figure 6b)	react.	2.3	2.2	1.9	2.1	3.27
	TS	18.1$^{\neq}$	18.0$^{\neq}$	19.1$^{\neq}$	18.1$^{\neq}$	2.25
	prod.	−7.0	−5.3	−4.3	−5.6	1.55
5 (Figure 6c)	react.	4.3	4.0	3.7	0.1	3.17
	TS	18.6$^{\neq}$	18.3$^{\neq}$	19.3$^{\neq}$	16.3$^{\neq}$	2.23
	prod.	−5.7	−4.3	−4.3	−5.4	1.55
5 (Figure 6d)	react.	11.5	11.2	11.2	6.6	3.15
	TS	28.1$^{\neq}$	27.6$^{\neq}$	28.1$^{\neq}$	24.0$^{\neq}$	2.24
	prod.	−7.2	−5.6	−5.4	−6.2	1.56

[a] react.: pentadienyl cation; TS: transition state; prod.: oxyallyl cation.

on the starting cationic intermediate in Equation (5) revealed that all conformers possessing an equatorially oriented 2-methyl group (Figure 6e–h) were highly energetic compared to the corresponding axially substituted ones ($\Delta G >$ 2.2 kcal mol^{-1}). For this reason, their contribution to the formation of the products could be considered negligible. As found for the unsubstituted heterocyclic derivatives (Equations (1) and (2)) the *N*-CO_2Me protection generates through rotation two initial conformers. Whatever starting conformer we consider, the DFT calculations resulted in path a (Figure 6a and c), that is, the formation of the new bond along the pseudoaxial direction, which is favored when compared to path b (Figure 6b and d). In the most favorable case (compare Figure 6a and b), the $\Delta\Delta G^{\neq}$ value is equal to 2.3 kcal mol^{-1}, with $\Delta G^{\neq}$ values of 15.7 and 18.1 kcal mol^{-1} for paths a and b, respectively, which means that at room temperature practically only the *cis* compound could be formed, in accordance to our experimental findings.[15d] In all cases, even if we consider the cyclization of the least-populated equatorial conformers, the most favored paths (Figure 6f and h) would always provide the *cis* diastereomer through a bond formation along a pseudoequatorial direction. This clearly emerges by comparing the energy profiles shown in Figure 6e and g with those in 6f and 6h, respectively. In contrast to what was reported by us for the analogous O derivatives,[18] the compared analysis of the TSs found along path a (Figure 6a) and b (Figure 6b) did not

clearly show that the pseudoaxial attack is favored by stereoelectronic reasons because, at the same isocontour level, the molecular orbital involved in the forming C5–C3′ bond had the same degree of completeness in the two TSs (data not shown). However, the pseudoaxial bond formation should be favored by the fact that it takes place on the opposite side of the axial 2-methyl substituent, whereas a pseudoequatorial attack could lead to steric hindrance with that group (Scheme 4b). Much chemistry has been indeed based on the axial preference of 2-alkyl substituents to the N atom of unsaturated piperidines bearing an electron-withdrawing N-protecting group and the way by which it strongly affects the stereochemical outcome of additions to the enamine double bond.[26]

Finally, we evaluated the energy profiles associated with the Nazarov reaction of thiopyranyl derivative **12b** (R^1 = Me), which under acidic conditions generates carbocation **13b** ($R^1 = R^2$ = Me, R^3 = Et) as the initial intermediate of the electrocyclization process (Equation (6), Figure 7, and Table 6). As in the case of the corresponding pyranyl derivative,[18] the 2-methyl group has a preferential equatorial orientation in intermediate **12b**, although the equatorial conformer is more stable only by 0.9 kcal mol^{-1} than the axial one, whereas this difference was 1.9 kcal mol^{-1} in the case of the O derivative. The electrocyclization again preferentially occurs along path a (Figure 7a and c), in which the new bond is formed along the pseudoaxial direction ($\Delta G^{\neq}$ = 13.5 and 13.48 kcal mol^{-1}). Path b is less favored (in both conformers) as the TSs have energies of 14.1 and 15.2 kcal mol^{-1}. Based on these calculations, we should expect that the reaction could occur at room temperature (given the $\Delta G^{\neq}$ values), providing a greater amount of the *trans* compound in the cyclization of **12b**. However, based on the relative populations of the initial intermediates and the differences in $\Delta G^{\neq}$ values, we should expect a *trans*/*cis* ratio lower than 10:1 as observed in the Nazarov reaction of the corresponding pyranyl derivative. Accordingly, subjecting the latter under the usual acidic conditions (Amberlyst 15 in dichloromethane at room temperature), we observed the complete disappearance of the starting material after 16 h with the formation of an inseparable 3:1 mixture of diastereomers.

Table 6. Energies and geometrical parameters for Equation (6). Energy values are in kcal mol^{-1}.[a]

Equation		ΔE_{elec}	$\Delta(E_{elec}$+ ZPVE)	$\Delta G_{gas\ phase}$	ΔG_{total}	C5–C3′ [Å]
6 (Figure 7a)	react.	1.0	1.1	1.3	0.9	3.09
	TS	13.9^{+}	13.8^{+}	15.1^{+}	13.5^{+}	2.20
	prod.	−7.3	−5.4	−4.2	−4.6	1.56
6 (Figure 7b)	react.	1.4	1.6	1.7	1.6	3.13
	TS	14.7^{+}	14.6^{+}	15.6^{+}	14.1^{+}	2.23
	prod.	−9.2	−7.3	−6.0	−6.6	1.56
6 (Figure 7c)	react.	0	0	0	0	3.09
	TS	13.0^{+}	12.7^{+}	13.7^{+}	13.4^{+}	2.20
	prod.	−9.1	−7.5	−6.6	−5.9	1.55
6 (Figure 7d)	react.	0.4	0.4	0.5	0.4	3.13
	TS	14.2^{+}	14.1^{+}	15.0^{+}	15.2^{+}	2.23
	prod.	−9.9	−8.3	−7.0	−6.0	1.56

[a] react.: pentadienyl cation; TS: transition state; prod.: oxyallyl cation.

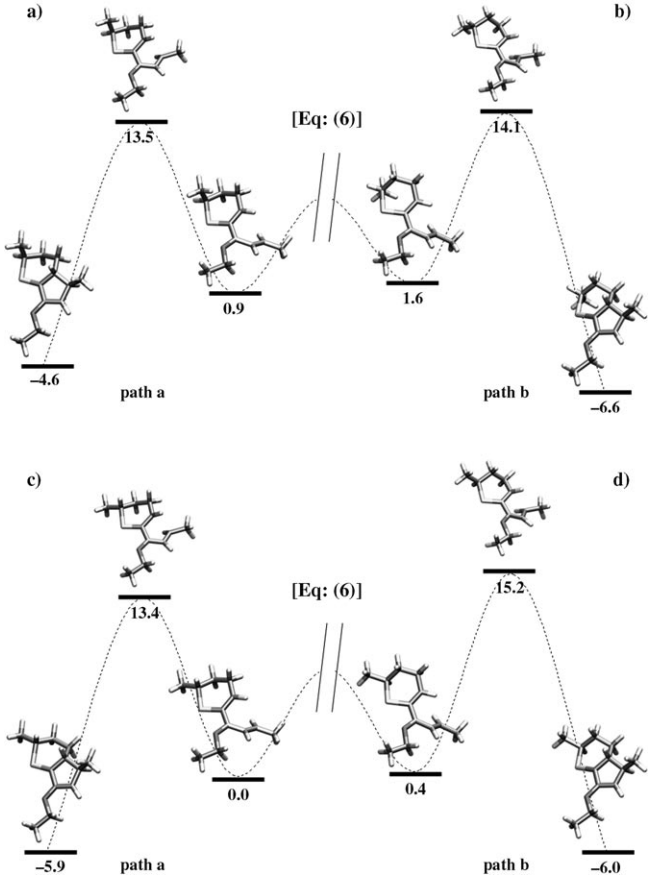

Figure 7. The free-energy profiles (in kcal mol^{-1}) for Equation (6). Four conformers (two axial (a–b) and two equatorial (c–d)) of the reactant were taken into account to explore all possible energy profiles. Paths a and b refer to Scheme 3.

Conclusion

We have demonstrated that DFT calculations are well suited to provide an in-depth understanding of the Nazarov reaction of pentadienyl cations generated by protonation of either dienones or alkoxytrienes. In particular, calculations at the DFT/B3LYP/6-311G** level of theory accurately predicted, and accounted for, both in terms of reactivity and torquoselectivity, the outcome of the Brønsted acid-catalyzed electrocyclization of 4π-electron systems in which one of the double bonds involved in the process is embedded in N- and S-heterocyclic rings. The findings of this study can be summarized as follows.

Effect of the heteroatom at C-6 on the reaction rate: Compared to the corresponding carbacyclic systems, a S atom at C-6 is capable of accelerating the reaction, whichever way the pentadienyl cation is generated, that is, by protonation of the corresponding dienone or the alkoxytriene. However,

slightly higher activation energies (15.3 vs. 13.4 kcal mol^{-1}) are associated with the electrocyclization of the dienones as the protonated starting intermediate is stabilized by an OH···S interaction. This difference of reactivity between dienone and alkoxytriene increases in the case of the analogous N derivative. Our calculations predicted that the dienones activation energies would be higher than 19 kcal mol^{-1} due to the strong hydrogen bond between the OH and the N-protecting group in the reacting pentadienyl cation, whereas in the cyclization of the ethoxytrienes, the activation energies decrease to 16 kcal mol^{-1}. Therefore, in general, alkoxytrienes are more reactive than the corresponding dienones under protic conditions. Repulsive steric interactions between the N-protecting group and the ethoxy group, which increase along the reaction profile from the starting intermediate to the TS, instead account for the higher activation energies generally found for the *N*-heterocyclic derivatives if compared to substrates substituted at C-6 by both sulfur and oxygen. Similarly to the latter, both the N and S atom at C-6 are capable of stabilizing the positive charge that develops on this carbon atom in the TSs, thus accounting for the higher reactivity of N- and S-substituted substrates relative to the carbacyclic dienones or ethoxytrienes. The consistency of the above DFT (and all the other herein reported) predictions about the reactivity with the experimental results, suggests that $\Delta G^{\neq}$ values, computed at the DFT/B3LYP/6-311G** level of theory, lower than 14 kcal mol^{-1} stand for fast reactions at room temperature, whereas $\Delta G^{\neq}$ values higher than 18 kcal mol^{-1} correspond to very slow reactions or reactions that do not occur at all under the same conditions.

Stereoselectivity in the ring closure: The DFT calculations showed that the formation of the new bond along a pseudoaxial direction is kinetically preferred. However, whether this was or was not due to a greater orbital overlap in the TS of path a when compared to the TS of path b could not be univocally demonstrated in the light of the present calculations for both N and S derivatives. Notably, this is in contrast to our previous computational results obtained with the pyranyl derivatives in which a greater orbital overlap was found in the pseudoaxial bond formation, which explained the *trans* stereoselectivity in the cyclization. When a protected N atom is present in the ring at C-6, the R^1 substituent in the ring is axially oriented to reduce the $A^{(1,3)}$ strain with the N-protecting group and the formation of the new bond along the axial direction leads to the 2,5-*cis* compounds. The exclusive formation of the *cis* compound we experimentally found is consistent with the activation energy difference of 2.3 kcal mol^{-1} found between the two competing pathways, which is reasonably due to the intervention of steric effects between the axial 2-methyl group and the forming C5–C3′ bond. As for the 2-alkyl-substituted S derivatives, small differences between equatorial and axial conformers of the pentadienyl cations, and between $\Delta G^{\neq}$ values, explain the low stereoselectivity in the ring closure.

In the light of the consistency observed between computational and experimental results, the usefulness of DFT calculations at the B3LYP/6-311G** level of theory as a robust instrument for the prediction of reactivity and stereoselectivity in such electrocyclic reactions is thus demonstrated.

Experimental Section

Computational methods: The gas-phase quantum chemical calculations were performed by using the Gaussian 03 (G03)[27] program suite. For all stationary points, both geometry and analytical frequency calculations were carried out at the DFT level of theory by using the restricted B3LYP hybrid functional,[28] which has already been successfully employed in the description of analogous pericyclic reactions.[9,20,29] The employed basis set was the Pople's 6-311G(d,p), which provides a single set of polarization functions both for the heavy atoms and the hydrogen atoms. Geometry optimizations were carried out in gas-phase by using the G03 default convergence criteria, by means of the Berny algorithm,[30] and the synchronous transit-guided quasi-Newton (STQN) method[31] (QST2 routine implemented in G03) for the local minima and saddle points, respectively. Frequency calculations at the reference T of 298.15 K were performed both to characterize stationary points and to calculate their thermodynamic properties. Since the present study focused on free-energy differences (relative free-energy values) between reactants and products and between reactants and saddle points, no scaling factors were applied on the computed zero-point vibrational energies. For all the reaction transition states hereafter reported, the diagonalized mass-weighted Hessian matrix showed only one negative eigenvalue, revealing a first-order saddle point. Moreover, for each identified saddle point, the corresponding normal mode (related to the negative eigenvalue) involved nuclear displacements along the investigated reaction coordinate. Besides, as a further piece of evidence for the proper reaction path, some intrinsic reaction calculations (IRC)[32,33] on selected systems were also carried out at the B3LYP/6-311G(d,p) level of theory (data not shown). Finally, the solvent contribution was assessed in all stationary points by means of the SMxGAUSS 2.0.1 program.[34] SMxGAUSS is a quantum mechanical package that performs liquid-phase calculations by using the SMx suite of universal solvation models developed by Truhlar and co-workers.[35] The latter is a set of continuum solvation models based on the generalized Born approximation, in which first-solvation effects are modeled with atomic surface tension functionals proportional to the solvent-accessible surface area (SASAs) of the atoms in the solute.[35] These functionals are parameterized to properly reproduce a wide set of free energies of solvation in water and in organic solvents. Notably, the SM5.43R universal model more accurately predicts both aqueous and organic free energy of solvation[35] than the framework of polarizable continuum model (PCM) methods.[36] Here, single-point self-consistent reaction-field (SCRF) calculations on the previously converged geometries were carried out in an implicit dichloromethane (CH_2Cl_2) continuum by using the SM5.43R solvation model. The mPW1K hybrid functional was chosen to describe the solute, as it has been suggested for calculating kinetics,[35] along with the 6-31G(d) basis set. Due to level of theory differences between the gas-phase calculations and the evaluation of the solvent contributions, the solvent correction to the free energies differences must be definitely intended as an independent addictive term. Briefly, the relative molar free energies were calculated as follows:

$$\Delta G_{\text{total}} = (\Delta G_{\text{gas phase}})^{\text{B3LYP/6-311G**}} + (\Delta G_{\text{solvation}})^{\text{mPW1K/6-31G*}}$$

The gas-phase free energy is defined as:

$$\Delta G_{\text{gas phase}} = \Delta E_{\text{elec}} + \Delta ZPE + \Delta H_{\text{vibr-rot}}(T) - T\Delta S(T)$$

in which ΔE_{elec}, ΔZPE, $\Delta H_{\text{vibr-rot}}(T)$, and $\Delta S(T)$ are the electronic energy, the zero-point energy, the vibrational-rotational enthalpy, and the total entropy calculated at 298.15 K, respectively. The solvation free energy

was calculated as follows:

$$\Delta G_{solvation} = \Delta E_{elec} + G_p + G_{CDS} + \Delta G_{vibr\text{-}rot}$$

in which ΔE_{elec} and $\Delta G_{vir\text{-}rot}$ are the solute changing in electronic energy and in vibrational-rotational free energy, respectively, following solvation, G_p is the electronic polarization energy, and G_{CDS} is a semiempirical term (see Thompson et al. for details[34]).

Some calculations were carried out by adding one electron to the systems to estimate the effects of the positive charge on both the reactants and the transition states (see the Results and Discussion). These calculations were carried out by using the restricted open-shell ROB3LYP functional (employing the same basis set as reported above), as the spin multiplicity passed from 1 to 2.

The partial charges were computed by following the standard two-stage RESP fitting procedure[37,38] fitting first the polar areas by using weak hyperbolic restraints (0.0005 a.u.), and then fitting the remaining areas imposing equivalencies and by imposing a stronger restraint (0.001 a.u.). The quantum electrostatic potential used was sampled by adapting the Merz–Kollman–Singh (MKS) scheme,[39,40] namely, by using 10 concentric layers at the default level of spacing, a surface density of 6 points $Å^{-2}$, and the default MKS van der Waals radii (as elsewhere suggested[41]).

For the intermediates of Equations (1–6), one of the two enantiomers was arbitrarily chosen for the study.

Metropolis Monte Carlo conformational searches were carried out at 300 K by using the MacroModel software package.[42] 10,000 conformers were generated and the Metropolis criterion was adopted to accept or discard any Monte Carlo move. All single bonds were left freely moving. The outcomes of Monte Carlo conformational searches were clusterized by means of AClAP,[43] by using the average linkage rule and the KGS penalty function. This protocol has been proved to be well-suited to conformational analysis of low-to-high conformationally complex small organic molecules.[43b]

All calculations were performed on a Linux cluster employing an open Mosix architecture.

General remarks: Chromatographic separations were performed under pressure on silica gel by using flash-column techniques; R_f values refer to TLC carried out on 0.25 mm silica gel plates with the same eluant indicated for the column chromatography. THF was distilled from Na/benzophenone. Dichloromethane was distilled from CaH_2. ^1H and ^{13}C NMR spectra were recorded on a Varian Gemini 200 (^1H: 200 MHz, ^{13}C: 50.33 MHz) or a JEOL Eclipse Plus 400 (^1H: 400 MHz) at 25 °C. The chemical shifts (δ) and coupling constants (J) are expressed in ppm and Hertz, respectively. Mass spectra were carried out by EI at 70 eV on a Shimadzu GC/MS QP5050 instrument. Triflates **16** and **17** were prepared as reported.[23] Compound **6b**[15b] and **11**[23] (Scheme 5) were prepared as reported. 2-(1-Ethoxybuta-1,3-dienyl)-5,5-dimethyl[1,3,2]dioxaborinane (**19**; Schemes 4 and 5) was prepared as reported.[44]

Methyl 6-[(1*E*)-1-ethoxybuta-1,3-dien-1-yl]-3,4-dihydropyridine-1(2*H*)carboxylate (7a): $[PdCl_2(Ph_3P)_2]$ (35 mg, 0.05 mmol), boronate **19** (210 mg, 1.0 mmol), and a 2 M aqueous K_2CO_3 solution (1 mL) were added to a solution of **16** (289 mg, 1.0 mmol) in THF (7 mL), under an argon atmosphere. The mixture was stirred for 0.5 h at room temperature. Water (25 mL) was then added, the mixture extracted with diethyl ether (3× 20 mL), and dried over K_2CO_3. Evaporation of the solvent afforded a yellow oil that was purified by chromatography (EtOAc/petroleum ether 1:5, 1% Et_3N, $R_f = 0.65$) to give **7a** (161 mg, 68% yield) as a pale-yellow oil. ^1H NMR (200 MHz, $CDCl_3$): $\delta = 6.53$ (dt, $^3J(H,H) = 16.8$, 10.4 Hz, 1H; $CH_2{=}CH{-}CH{=}C(OEt)$), 5.40 (d, $^3J(H,H) = 10.4$ Hz, 1H; $CH_2{=}CH{-}CH{=}C(OEt)$), 5.32 (t, $J = 3.7$ Hz, 1H; H-5), 4.99 (dd, $^3J(H,H) = 16.8$, $^2J(H,H) = 1.1$ Hz, 1H; $CH_2{=}CH{-}CH{=}C(OEt)$), 4.77 (dd, $^3J(H,H) = 10.4$, $^2J(H,H) = 1.1$ Hz, 1H; $CH_2{=}CH{-}CH{=}C(OEt)$), 3.79 (q, $^3J(H,H) = 7.1$ Hz, 2H; OCH_2CH_3), 3.65 (s, 3H; CO_2Me), 3.70–3.60 (m, 2H; CH_2N), 2.21–2.18 (m, 2H; 4-H, 4-H′), 1.96–1.73 (m, 2H; 3-H, 3-H′), 1.27 ppm (t, $^3J(H,H) = 7.1$ Hz, 3H; OCH_2CH_3); ^{13}C NMR (50.33 MHz, $CDCl_3$): $\delta =$ 156.0 (s; CO_2Me), 155.9 (s; $C(OEt)$), 133.6 (d; $CH_2{=}CH{-}$), 133.1 (s; C-6), 118.4 (d; C-5), 111.0 (t; $CH_2{=}CH{-}$), 103.6 (d; $C(OEt){=}C$), 63.5 (t; C-2), 52.4 (q; OCH_3), 43.7 (t; OCH_2CH_3), 23.0 (t; C-4), 22.9 (t; C-3), 14.5 ppm (q); MS (70 eV, EI): m/z (%): 237 (85) $[M]^+$, 208 (100), 176 (75), 148 (45), 136 (48); elemental analysis calcd (%) for $C_{13}H_{19}NO_3$: C 65.80, H 8.07, N 5.90; found: C 65.67, H 7.91, N 5.78.

Methyl 5-methyl-7-oxo-2,3,4,5,6,7-hexahydro-1*H*-cyclopenta[b]pyridine-1-carboxylate (10a): Amberlyst 15 (16 mg) was added to a solution of **7a** (118 mg, 0.5 mmol) in anhydrous CH_2Cl_2 (5 mL) under an argon atmosphere, and the resulting mixture was stirred at room temperature. The reaction was monitored by TLC and after 18 h, the resin was filtered off through a short pad of $NaHCO_3$ and the solution concentrated under vacuum. Crude products were purified by flash chromatography (AcOEt/petroleum ether 1:3, 0.5% Et_3N, $R_f = 0.45$) to give pure **10a** (56 mg, 54%). ^1H NMR (200 MHz, $CDCl_3$): $\delta = 3.75$ (s, 3H; CO_2Me), 3.65–3.50 (m, 2H; CH_2N), 2.72 (m, 1H; 5-H), 2.66 (dd, $^2J(H,H) = 15.9$, $^3J(H,H) =$ 6.7 Hz, 1H; 6-H), 2.47 (dt, $^2J(H,H) = 19.8$, $^3J(H,H) = 6.3$ Hz, 1H; 4-H), 2.20 (dt, $^2J(H,H) = 19.8$, $^3J(H,H) = 6.5$ Hz, 1H; 4-H′), 2.01 (d, $^2J(H,H) =$ 15.9 Hz, 1H; 6-H′), 1.87–1.80 (m, 2H; 3-H, 3-H′), 1.17 ppm (d, $^3J(H,H) =$ 7.0 Hz, 3H; CCH_3); ^{13}C NMR (50.33 MHz, $CDCl_3$): $\delta = 198.7$ (s; C-7), 161.5 (s; CO_2Me), 137.9 (s; C-7a), 131.4 (s; C-4a), 53.1 (q; OCH_3), 44.1 (t; C-2), 42.8 (t; C-6), 33.3 (d; C-5), 23.9 (t; C-4), 22.2 (t; C-3), 19.1 ppm (q; CCH_3); MS (70 eV, EI): m/z (%): 209 (100) $[M]^+$, 195 (73), 193 (55), 152 (60), 149 (90), 121 (63), 106 (60), 92 (52); elemental analysis calcd (%) for $C_{11}H_{15}NO_3$: C 63.14, H 7.23, N 6.69; found: C 63.00, H 7.51, N 6.44.

(1*E*)-1-(3,4-Dihydro-2*H*-thiopyran-6-yl)buta-1,3-dien-1-yl ethyl ether (12a): $[PdCl_2(Ph_3P)_2]$ (35 mg, 0.05 mmol), boronate **19** (210 mg, 1.0 mmol), and a 2 M aqueous K_2CO_3 solution (1 mL) were added to a solution of **17** (248 mg, 1.0 mmol) in THF (7 mL), under an argon atmosphere. The mixture was stirred for 0.5 h at room temperature. Water (25 mL) was then added, the mixture extracted with diethyl ether (3× 20 mL), and dried over K_2CO_3. Evaporation of the solvent afforded a yellow oil which was purified by chromatography (EtOAc/petroleum ether 1:9, 1% Et_3N, $R_f = 0.80$) to give **12a** (141 mg, 72%) as a pale-yellow oil. ^1H NMR (200 MHz): $\delta = 6.57$ (td, $^3J(H,H) = 16.8$, 10.2 Hz, 1H; $CH_2{=}CH{-}CH{=}C(OEt)$), 5.85 (t, $^3J(H,H) = 4.3$ Hz, 1H; 5-H), 5.41 (d, $^3J(H,H) = 10.2$ Hz, 1H; $CH_2{=}CH{-}CH{=}C(OEt)$), 5.03 (d, $^3J(H,H) =$ 16.8 Hz, 1H; $CH_2{=}CH{-}CH{=}C(OEt)$), 4.82 (d, $^3J(H,H) = 10.2$ Hz, 1H; $CH_2{=}CH{-}CH{=}C(OEt)$), 3.82 (q, $^3J(H,H) = 6.9$ Hz, 2H; OCH_2CH_3), 2.98–2.88 (m, 2H; CH_2S), 2.29–2.25 (m, 2H; 4-H, 4-H′), 2.10–2.05 (m, 2H; 3-H, 3-H′), 1.31 ppm (t, $^3J(H,H) = 6.9$ Hz, 3H; OCH_2CH_3); ^{13}C NMR (50.33 MHz, $CDCl_3$): $\delta = 156.9$ (s; $C(OEt)$), 133.6 (s; C-6), 127.5 (d; $CH_2{=}CH{-}$), 124.2 (d; C-5), 111.8 (t; $CH_2{=}CH{-}$), 104.0 (d; $C(OEt){=}C$), 63.4 (t; OCH_2CH_3), 26.9 (t; C-2), 24.0 (t; C-4), 21.6 (t; C-3), 14.4 ppm (q; OCH_2CH_3); MS (70 eV, EI): m/z (%): 196 (100) $[M]^+$, 167 (85), 139 (70), 105 (65), 79 (95); elemental analysis calcd (%) for $C_{11}H_{16}OS$: C 67.30, H 8.22; found: C, 66.41; H 7.99.

5-Methyl-3,4,5,6-tetrahydrocyclopenta[b]thiopyran-7(2*H*)one (15a): Amberlyst 15 (16 mg) was added to a solution of (1-ethoxybuta-1,3-dienyl)-3,4-dihydro-2*H*-thiopyran (**12a**; 98 mg, 0.5 mmol) in anhydrous CH_2Cl_2 (5 mL) under an argon atmosphere, and the resulting mixture was stirred at room temperature. The reaction was monitored by TLC and after 4 h, the resin was filtered off through a short pad of $NaHCO_3$ and the solution concentrated under vacuum. Crude products were purified by flash chromatography (AcOEt/petroleum ether 1:4, 0.5% Et_3N, $R_f = 0.4$) to give pure **15a** (55 mg, 66%). ^1H NMR (200 MHz, $CDCl_3$): $\delta = 2.95$–2.74 (m, 2H, 1H; CH_2S, 5-H), 2.74–2.25 (m, 2H, 1H; 4-H, 4-H′, 6-H), 2.00 (d, $^2J(H,H) = 19.0$ Hz, 1H; 6-H′), 2.05–1.95 (m, 2H; 3-H, 3-H′), 1.17 ppm (d, $^3J(H,H) = 7.0$ Hz, 3H; CCH_3); ^{13}C NMR (50.33 MHz, $CDCl_3$): $\delta = 204.1$ (s; C-7), 167.8 (s; C-7a), 132.5 (s; C-4a), 42.3 (t; C-6), 37.9 (d; C-5); 25.2 (t; C-2, C-4), 22.1 (t, C-3), 18.7 ppm (q, CH_3); MS (70 eV, EI): m/z: 168 (100) $[M]^+$, 153 (100), 139 (25), 97 (23); elemental analysis calcd (%) for $C_9H_{12}OS$: C 64.25, H7.19; found: C 64.40, H 7.15.

5-Propyl-3,4,5,6-tetrahydrocyclopenta[b]thiopyran-7(2*H*)one (15b): Amberlyst 15 (6 mg) was added to a solution of **11** (25 mg, 0.13 mmol) in anhydrous CH_2Cl_2 (1.5 mL) under an argon atmosphere, and the resulting mixture was stirred at room temperature. The reaction was monitored by TLC and after 24 h, the resin was filtered off through a short pad of $NaHCO_3$ and the solution concentrated under vacuum. The ratio be-

tween **15b** (59%) and **11** (41%) was determined by ^{1}H NMR spectroscopic analysis of the crude reaction mixture. This was then purified by flash chromatography (EtOAc/petroleum ether 1:8, 0.5% Et_3N, $R_f = 0.28$) to give pure **15b** (14 mg) in 55% yield. Spectroscopic data of **15b** are identical to those reported.[15a]

2-Methyl-3,4-dihydro-2*H*-thiopyran-6-yl trifluoromethanesulfonate (18)

*Preparation of 6-methyltetrahydro-2*H*-thiopyran-2-one*: This was prepared according to a slight modification of the reported procedure.[45] A mixture of 6-methyltetrahydropyran-2-one (15 mmol), thiourea (1.1 g, 15 mmol), and hydrobromidric acid (2 mL, 48%) was refluxed whilst stirring (6 h). After cooling, NaOH (2 g) in water (2 mL) was added and the mixture was refluxed again under nitrogen for 2 h. The cooled solution was extracted with ether and the ether extracts discarded. The aqueous residue was acidified to pH 1 with concentrated hydrocloridric acid and extracted with ether. The extracts were dried over sodium K_2CO_3 and the solvent removed. The residue was then diluted with 25 mL of toluene and refluxed for 1 h in the presence of catalytic *p*-toluene sulfonic acid. After cooling, the organic layer was washed with water, dried over K_2CO_3, and the solvent removed. The oil obtained was purified by distillation. B.p. 85 °C (12 mm Hg); yield: 85%; ^{1}H NMR (200 MHz, $CDCl_3$): $\delta = 3.54$ (m, 1H), 2.57 (dt, $J = 17.5$, 5.0 Hz, 1H), 2.42 (ddd, $J = 17.5$, 10.5, 5.4 Hz, 1H), 2.15 (m, 1H), 2.02 (m, 1H), 1.82 (m, 1H), 1.53 (m, 1H), 1.31 ppm (d, $J = 6.7$ Hz, 3H); ^{13}C NMR (50.33 MHz, $CDCl_3$): $\delta = 202.0$ (s), 40.8 (d), 40.4 (t), 32.1 (t), 22.3 (q), 22.0 ppm (t).

Preparation of the triflate: The above 6-methyl-tetrahydrothiopyran-2-one (158 mg, 1.21 mmol) in THF (4 mL) was added to a solution of potassium hexamethyldisilazide (3.16 mL, 1.58 mmol) in THF (5 mL) at −78 °C. After 1 h, *N*-phenyltrifluoromethansulfonimide (392 mg, 1.10 mmol) in THF (5 mL) was added. The mixture was stirred at −78 °C for 1 h, and then the temperature was raised to room temperature for 6 h. Water (20 mL) was added and the mixture was extracted with Et_2O. The organic layer was then washed with NaOH 10% and brine. After evaporation of the solvent, the crude product **18** (274 mg, 85%) was obtained and used without further purification. ^{1}H NMR (200 MHz, $CDCl_3$): $\delta = 5.84$ (t, ^3J(H,H) = 4.4 Hz, 1H; 5-H), 3.59 (m, 1H; 2-H), 2.55–2.45 (m, 2H; 4-H, 4-H′), 2.02–1.85 (m, 2H; 3-H, 3-H′), 1.38 ppm (d, ^3J(H,H) = 6.8 Hz, 3H; CH_3).

6-[(1*E*)-1-Ethoxybuta-1,3-dien-1-yl]-2-methyl-3,4-dihydro-2*H*-thiopyran (12c): $[PdCl_2(Ph_3P)_2]$ (35 mg, 0.05 mmol), 2-(1-ethoxybuta-1,3-dienyl)-5,5-dimethyl-[1,3,2]dioxaborinane (**19**; 210 mg, 1.0 mmol), and a 2 M aqueous K_2CO_3 solution (1 mL) were added to a solution of crude triflate **18** (262 mg, 1.0 mmol) in THF (7 mL), under an argon atmosphere. The mixture was stirred for 0.5 h at room temperature. Water (25 mL) was then added, the mixture was extracted with diethyl ether (3 × 20 mL) and dried over K_2CO_3. Evaporation of the solvent afforded a yellow oil which was purified by chromatography (EtOAc/petroleum ether 1:9, 1% Et_3N, $R_f = 0.85$) to give **12c** (143 mg, 68%) as a pale-yellow oil. ^{1}H NMR (200 MHz, $CDCl_3$): $\delta = 6.56$ ppm (td, ^3J(H,H) = 17.0, 10.4 Hz, 1H; CH_2=C*H*−CH=C(OEt)), 5.85 (dd, ^3J(H,H) = 3.9, 4.7 Hz, 1H; 5-H), 5.42 (d, ^3J(H,H) = 10.4 Hz, 1H; CH_2=CH−C*H*=C(OEt)), 5.04 (dd, ^3J(H,H) = 17.0, ^2J(H,H) = 2.0 Hz, 1H; CH_2=CH−CH=C(OEt)), 4.83 (dd, ^3J(H,H) = 10.4, ^2J(H,H) = 2.0 Hz, 1H; CH_2=CH−CH=C(OEt)), 3.83 (q, ^3J(H,H) = 7.0 Hz, 2H; OCH_2CH$_3$) 3.25 (dqd, ^3J(H,H) = 2.5, 6.8, 9.8 Hz, 1H; C*H*S), 2.45–2.30 (m, 2H; 4-H, 4-H′), 2.05–2.25 (m, 2H; 3-H, 3-H′), 1.69 (t, ^3J(H,H) = 7.0 Hz, 3H; OCH$_2$CH_3), 1.34 ppm (d, ^3J(H,H) = 6.8 Hz, 3H; CH_3); ^{13}C NMR (50.33 MHz, $CDCl_3$): $\delta = 156.9$ (s; *C*(OEt)), 133.7 (s; C-6), 127.8 (d; CH_2=*C*H−), 123.6 (d; C-5), 111.9 (t; *C*H$_2$=CH−), 104.8 (d; C-(OEt)=*C*), 63.4 (t; OCH$_2$CH$_3$), 35.6 (d; C-2), 30.3 (t; C-4), 24.4 (t; C-3), 21.0 (q; *C*H$_3$), 14.5 ppm (q; OCH$_2$*C*H$_3$); MS (70 eV, EI): *m*/*z*: 210 (100) $[M]^+$, 181 (75), 139 (25), 55 (21); elemental analysis calcd (%) for $C_{12}H_{18}OS$: C 68.52, H 8.63; found: C 68.32, H, 8.51.

2,5-Dimethyl-3,4,5,6-tetrahydrocyclopenta[b]thiopyran-7(2*H*)one (15c): Amberlyst 15 (2.3 equiv g^{-1}, 10 mg) was added to a solution of **12c** (72 mg, 0.34 mmol) in anhydrous CH_2Cl_2 (5 mL) under an argon atmosphere, and the resulting mixture was stirred at room temperature. The reaction was monitored by TLC and after 4 h, the resin was filtered off through a short pad of $NaHCO_3$ and the solution concentrated under vacuum. Crude products were purified by flash chromatography (AcOEt/petroleum ether 1:4, 0.5% Et_3N, $R_f = 0.4$) to give **15c** (49 mg, 79%) as a 3:1 diastereomeric mixture. ^{1}H NMR (400 MHz, $CDCl_3$): major diastereomer: $\delta = 3.25$–3.10 (m, 1H; C*H*S), 2.93–2.72 (m, 1H; 5-H), 2.65 (dd, ^2J(H,H) = 17.4, ^3J(H,H) = 6.5 Hz; 6-H), 2.60–2.47 (m, 1H; 4-H), 2.45–2.32 (m, 1H; 4-H′), 2.27–2.13 (m, 1H; 3-H), 1.97 (dd, ^2J(H,H) = 17.4, ^3J(H,H) = 0.9 Hz, 1H; 6-H′), 1.85–1.70 (m, 1H; 3-H′), 1.29 (d, ^3J(H,H) = 6.8 Hz, 3H; CH_3), 1.12 ppm (d, ^3J(H,H) = 7.0 Hz, 3H; CH_3); ^{13}C NMR (50.33 MHz, $CDCl_3$): $\delta = 203.9$ (s, C-7), 167.3 (s, C-7a), 133.3 (s, C-4a), 42.7 (t, C-6), 37.8 (d, C-5), 34.7 (d, C-2), 30.7 (t, C-4), 25.5 (t, C-3), 20.8 (q, 2-*C*H$_3$), 18.7 ppm (q, *C*H$_3$); MS (70 eV, EI): *m*/*z*: 182 (100) $[M]^+$, 167 (100), 154 (25), 97 (23); elemental analysis calcd (%) for $C_{10}H_{14}OS$: C 65.89, H 7.74; found: C 65.40, H 7.45.

Acknowledgements

The authors wish to thank Mrs. B. Innocenti and Mr. M. Passaponti for technical assistance. MIUR-COFIN is gratefully acknowledged for financial support.

[1] *Comprehensive Organic Synthesis, Vol. 5* (Eds.: B. M. Trost, I. Fleming; Vol. Ed.: L. A. Paquette), Pergamon Press, Oxford, **1991**.
[2] I. Fleming, *Pericyclic Reactions*; Oxford University Press, Oxford, **2004**.
[3] F. L. Ansari, R. Qureshi, M. L. Qureshi, *Electrocyclic Reactions, From Fundamentals to Research*, Wiley-VCH, Weinheim, **1999**.
[4] a) K. N. Houk, in *Strain and Its Implications in Organic Chemistry* (Eds.: A. de Meijere, S. Blechert), Kluwer Academic Publishers, Boston, **1989**, pp. 25–37; b) A. B. Buda, Y. Wang, K. N. Houk, *J. Org. Chem.* **1989**, *54*, 2264–2266.
[5] a) P. S. Lee, X. Zhang, K. N. Houk, *J. Am. Chem. Soc.* **2003**, *125*, 5072–5079; b) M. Murakami, Y. Miyamoto, Y. Ito, *Angew. Chem.* **2001**, *113*, 182–184; *Angew. Chem. Int. Ed.* **2001**, *40*, 189–190; c) M. J. Walker, B. N. Hietbrink, B. E. Thomas IV, K. Nakamura, E. A. Kallel, K. N. Houk, *J. Am. Chem. Soc.* **2001**, *123*, 6669–6672; d) S. Niwayama, E. A. Kallel, D. C. Spellmeyer, C. Sheu, K. N. Houk, *J. Org. Chem.* **1996**, *61*, 2813–2825; e) S. Niwayama, E. A. Kallel, C. Sheu, K. N. Houk, *J. Org. Chem.* **1996**, *61*, 2517–2522; f) W. R. Dolbier, Jr, H. Koroniak, K. N. Houk, C. Sheu, *Acc. Chem. Res.* **1996**, *29*, 471–477; g) C. W. Jefford, G. Bernardinelli, Y. Wang, D. C. Spellmeyer, A. Buda, K. N. Houk, *J. Am. Chem. Soc.* **1992**, *114*, 1157–1165; h) J. D. Evanseck, B. E. Thomas IV, K. N. Houk, *J. Org. Chem.* **1995**, *60*, 7134–7141; i) K. Nakamura, K. N. Houk, *J. Org. Chem.* **1994**, *60*, 686–691; j) W. Kirmse, N. G. Rondan, K. N. Houk, *J. Am. Chem. Soc.* **1984**, *106*, 7989–7991.
[6] a) D. A. Smith, C. W. Ulmer II, *J. Org. Chem.* **1993**, *58*, 4118–4121; b) D. A. Smith, C. W. Ulmer II, *J. Org. Chem.* **1997**, *62*, 5110–5115; c) D. A. Smith, C. W. Ulmer II, *Tetrahedron Lett.* **1991**, *32*, 725–728.
[7] S. E. Denmark, M. A. Wallace, C. B. Walker, *J. Org. Chem.* **1990**, *55*, 5543–5545.
[8] E. A. Kallel, K. N. Houk, *J. Org. Chem.* **1989**, *54*, 6006–6008.
[9] a) L. O. N. Faza, C. S. López, R. Álvarez, Á. R. de Lera, *Chem. Eur. J.* **2004**, *10*, 4324–4333.
[10] M. Harmata, P. R. Schreiner, D. R. Lee, P. L. Kirchhoefer, *J. Am. Chem. Soc.* **2004**, *126*, 10954–10957.
[11] S. M. Bachrach, *Computational Organic Chemistry*, Wiley-Interscience, Hoboken, NJ, **2007**.
[12] For some recent examples of applications of the Nazarov reaction in the synthesis of natural products, see: a) W. He, J. Huang, X. Sun, A. J. Frontier, *J. Am. Chem. Soc.* **2008**, *130*, 300–308; b) D. R. Williams, L. A. Robinson, L. A. Nevill, J. P. Reddy, *Angew. Chem.* **2007**, *119*, 933–936; *Angew. Chem. Int. Ed.* **2007**, *46*, 915–918; c) G. X. Liang, Y. Xu, I. B. Seiple, D. Trauner, *J. Am. Chem. Soc.* **2006**, *128*, 11022–11023; d) G. O. Berger, M. A. Tius, *J. Org. Chem.* **2007**, *72*, 6473–6480; e) L. F. Wan, M. A. Tius, *Org. Lett.* **2007**, *9*, 647–650; f) E. G. Occhiato, C. Prandi, A. Ferrali, A. Guarna, *J. Org. Chem.* **2005**, *70*, 4542–4545; reviews on the Nazarov reaction: g) K. L.

Habermas, S. E. Denmark, T. D. Jones, *Org. React.* **1994**, *45*, 1–158; h) S. E. Denmark, in *Comprehensive Organic Synthesis, Vol. 5* (Eds.: B. M. Trost, I. Fleming; Vol. Ed.: L. A. Paquette), Pergamon Press, Oxford, **1991**, pp. 751–784; i) M. A. Tius, *Eur. J. Org. Chem.* **2005**, 2193–2206; j) H. Pellissier, *Tetrahedron* **2005**, *61*, 6479–6517; k) A. J. Frontier, C. Collison, *Tetrahedron* **2005**, *61*, 7577–7606.

[13] M. Rueping, W. Ieawsuwan, A. P. Antonchick, B. J. Nachtstein, *Angew. Chem.* **2007**, *119*, 2143–2146; *Angew. Chem. Int. Ed.* **2007**, *46*, 2097–2100.

[14] a) W. He, I. Herrick, T. A. Atesin, P. A. Caruana, C. A. Kallenberger, A. J. Frontier, *J. Am. Chem. Soc.* **2008**, *130*, 1003–1011; b) W. He, J. Huang, X. Sun, A. J. Frontier, *J. Am. Chem. Soc.* **2007**, *129*, 489–499; c) J. A. Malona, J. M. Colbourne, A. J. Frontier, *Org. Lett.* **2006**, *8*, 5661–5664; d) M. Janka, M. He, A. J. Frontier, C. Flaschenriem, R. Eisenberg, *Tetrahedron* **2005**, *61*, 6193–6206; e) M. Janka, W. He, A. J. Frontier, R. Eisenberg, *J. Am. Chem. Soc.* **2004**, *126*, 6864–6865; f) W. He, X. Sun, A. J. Frontier, *J. Am. Chem. Soc.* **2003**, *125*, 14278–14279.

[15] a) L. Bartali, P. Larini, A. Guarna, E. G. Occhiato, *Synthesis* **2007**, 1733–1737; b) P. Larini, A. Guarna, E. G. Occhiato, *Org. Lett.* **2006**, *8*, 781–784; c) C. Prandi, A. Deagostino, P. Venturello, E. G. Occhiato, *Org. Lett.* **2005**, *7*, 4345–4348; d) E. G. Occhiato, C. Prandi, A. Ferrali, A. Guarna, P. Venturello, *J. Org. Chem.* **2003**, *68*, 9728–9741; e) E. G. Occhiato, C. Prandi, A. Ferrali, A. Guarna, A. Deagostino, P. Venturello, *J. Org. Chem.* **2002**, *67*, 7144–7146.

[16] a) G. Liang, D. Trauner, *J. Am. Chem. Soc.* **2004**, *126*, 9544–9545; b) G. Liang, S. N. Gradl, D. Trauner, *Org. Lett.* **2003**, *5*, 4931–4934.

[17] C. Prandi, A. Ferrali, A. Guarna, P. Venturello, E. G. Occhiato, *J. Org. Chem.* **2004**, *69*, 7705–7709.

[18] A: Cavalli, M. Masetti, M. Recanatini, C. Prandi, A. Guarna, E. G. Occhiato, *Chem. Eur. J.* **2006**, *12*, 2836–2845.

[19] For example: a) H. Drautz, H. Zähner, E. Kupfer, W. Keller-Schierlein, *Helv. Chim. Acta*, **1981**, *64*, 1752–1765; b) S. Grabley, H. Kluge, H.-U. Hoppe, *Angew. Chem.* **1987**, *99*, 692–693; *Angew. Chem. Int. Ed. Engl.* **1987**, *26*, 664–665; c) S. Grabley, P. Hammann, H. Kluge, J. Wink, P. Kricke, A. Zeek, *J. Antibiot.* **1991**, *44*, 797–800; d) C. Puder, P. Krastel, A. Zeeck, *J. Nat. Prod.* **2000**, *63*, 1258–1260; e) C. Puder, S. Loya, A. Hizi, A. Zeeck, *J. Nat. Prod.* **2001**, *64*, 42–45; f) B. M. Trost, C. K. Chung, A. B. Pinkerton, *Angew. Chem.* **2004**, *116*, 4427–4429; *Angew. Chem. Int. Ed.* **2004**, *43*, 4327–4329; g) S. Omura, H. Tanaka, J. Awaya, Y. Narimatsu, Y. Konda, T. Hata, *Agric. Biol. Chem.* **1974**, *38*, 899–906; h) A. I. Gurevich, M. N. Kolosov, V. G. Korobko, V. V. Onoprienko, *Tetrahedron Lett.* **1968**, *9*, 2209–2212; i) S. J. Bamford, T. Luker, W. N. Speckamp, H. Hiemstra, *Org. Lett.* **2000**, *2*, 1157–1160; j) C. H. Heathcock, M. H. Norman, D. A. Dickman, *J. Org. Chem.* **1990**, *55*, 798–811; k) L. E. Overman, G. M. Robertson, A. J. Robichaud, *J. Am. Chem. Soc.* **1991**, *113*, 2598–2610; l) L. E. Overman, M. Sworin, L. Bass, J. Clardy, *Tetrahedron* **1981**, *37*, 4041–4045; related and proline-specific Maillard compounds: m) C.-W. Chen, G. Lu, C.-T. Ho, *J. Agric. Food Chem.* **1997**, *45*, 2996–2999.

[20] a) V. Polo, J. Andrés, *J. Chem. Theory Comput.* **2007**, *3*, 816–823; b) F.-Q. Shi, X. Li, Y. Xia, L. Zhang, Z.-X. Yu, *J. Am. Chem. Soc.* **2007**, *129*, 15503–15512.

[21] Conditions used for carrying out the Nazarov reaction under Brønsted acidic conditions: CH_2Cl_2 as a solvent in the presence of catalytic amounts of the acidic resin Amberlyst 15 (32 mg per mmol of substrate).

[22] The OH···S hydrogen bond is known, for example, see: a) S. Millefiori, A. Millefiori, *J. Chem. Soc. Faraday Trans. 2* **1989**, *85*, 1465–1475; b) H. Yoshida, T. Harada, T. Murase, K. Ohno, H. Matsuura, *J. Phys. Chem. A* **1997**, *101*, 1731–1737.

[23] L. Bartali, A. Guarna, P. Larini, E. G. Occhiato, *Eur. J. Org. Chem.* **2007**, 2152–2163.

[24] a) We prepared *n*-propyl-substituted dienone **6b** (R^1=H, R^2=*n*Pr) instead of the corresponding methyl-substituted dienone **6a** (R^1=H, R^2=Me) as the 1-propenylboronic acid was commercially available. However calculations were carried out on **6a** as this has a more restricted conformational space. b) As suggested by one referee, we subjected to the usual Nazarov reaction conditions also the corresponding C3′-unsubstituted (i.e., lacking the *n*-propyl chain) dienone, but again no formation of the product was observed (degradation of the starting material instead took place).

[25] This result is consistent with our previous findings on the failed electrocyclization of differently N-protected (*N*-Cbz) dienones analogous to **6**. See reference [15d].

[26] a) T. Momose, N. Toyooka, *J. Org. Chem.* **1994**, *59*, 943–945, and references therein; b) D. L. Comins, S. P. Joseph, in *Advances in Nitrogen Heterocycles, Vol. 2* (Ed.: C. J. Moody) JAI Press, Greenwich, CT, **1996**, pp. 251–294; c) J. T. Kuethe, C. A. Brooks, D. L. Comins, *Org. Lett.* **2003**, *5*, 321–323; d) J. D. Ha, C. H. Kang, K. A. Belmore, J. K. Cha, *J. Org. Chem.* **1998**, *63*, 3810–3811; e) N. Toyooka, M. Okumura, H. Takahata, H. Nemoto, *Tetrahedron* **1999**, *55*, 10673–10684; f) T. Luker, H. Hiemstra, W. N. Speckamp, *J. Org. Chem.* **1997**, *62*, 3592–3596.

[27] Gaussian 03 (Revision B.05), M. J. Frisch, G. W. Trucks, H. B. Schlegel, G. E. Scuseria, M. A. Robb, J. R. Cheeseman, V. G. Zakrzewski, J. A. Montgomery, Jr., R. E. Stratmann, J. C. Burant, S. Dapprich, J. M. Millam, A. D. Daniels, K. N. Kudin, M. C. Strain, O. Farkas, J. Tomasi, V. Barone, M. Cossi, R. Cammi, B. Mennucci, C. Pomelli, C. Adamo, S. Clifford, J. Ochterski, G. A. Petersson, P. Y. Ayala, Q. Cui, K. Morokuma, D. K. Malick, A. D. Rabuck, K. Raghavachari, J. B. Foresman, J. Cioslowski, J. V. Ortiz, B. B. Stefanov, G. Liu, A. Liashenko, P. Piskorz, I. Komaromi, R. Gomperts, R. L. Martin, D. J. Fox, T. Keith, M. A. Al-Laham, C. Y. Peng, A. Nanayakkara, C. Gonzalez, M. Challacombe, P. M. W. Gill, B. G. Johnson, W. Chen, M. W. Wong, J. L. Andres, M. Head-Gordon E. S. P. Replogle, J. A. Pople, Gaussian, Inc., Pittsburgh, PA, **2003**.

[28] A. D. Becke, *J. Chem. Phys.* **1993**, *98*, 1372–1377.

[29] B. Iglesias, À. R. de Lera, J. Rodríguez-Otero, S. López, *Chem. Eur. J.* **2000**, *6*, 4021–4033.

[30] C. Peng, P. Y. Ayala, H. B. Schlegel, M. J. Frisch, *J. Comput. Chem.* **1996**, *17*, 49–56.

[31] C. Peng, H. B. Schlegel, *Isr. J. Chem.* **1993**, *33*, 449–454.

[32] C. Gonzalez, H. B. Schlegel, *J. Chem. Phys.* **1989**, *90*, 2154–2161.

[33] C. Gonzalez, H. B. Schlegel, *J. Phys. Chem.* **1990**, *94*, 5523–5527.

[34] J. D. Thompson, C. J. Cramer, D. G. Truhlar, *J. Phys. Chem. A* **2004**, *108*, 6532.

[35] J. D. Thompson, C. J. Cramer, D. G. Truhlar, *Theor. Chem. Acc.* **2005**, *113*, 107–131.

[36] S. Miertus, E. Scrocco, J. Tomasi, *Chem. Phys.* **1981**, *55*, 117–129.

[37] C. I. Bayly, P. Cieplak, W. D. Cornell P. A. Kollman, *J. Phys. Chem.* **1993**, *97*, 10269–10280.

[38] W. D. Cornell, P. Cieplak, C. I. Bayly, P. A. Kollman, *J. Am. Chem. Soc.* **1993**, *115*, 9620–9631.

[39] U. C. Singh, P. A. Kollman, *J. Comput. Chem.* **1983**, *5*, 129–145.

[40] B. H. Besler, K. M. Merz, P. A. Kollman, *J. Comput. Chem.* **1990**, *11*, 431–439.

[41] E. Sigfridsson, U. Ryde, *J. Comput. Chem.* **1998**, *19*, 377–395.

[42] F. Mohamadi, N. G. J. Richards, W. C. Guida, R. M. J. Liskamp, M. A. Lipton, C. E. Caulfield, G. Chang, T. F. Hendrickson, W. C. Still, *J. Comput. Chem.* **1990**, *1*, 440–467.

[43] a) G. Bottegoni, W. Rocchia, M. Recanatini, A. Cavalli, *Bioinformatics* **2006**, *22*, e58–e65; b) G. Bottegoni, A. Cavalli, M. Recanatini, *J. Chem. Inf. Model.* **2006**, *46*, 852–862.

[44] P. Balma Tivola, A. Deagostino, C. Prandi, P. Venturello, *Org. Lett.* **2002**, *4*, 1275–1277.

[45] I. Roling, H.-G. Schamrr, W. Eisenreich, K.-H. Engel, *J. Agric. Food Chem.* **1998**, *46*, 668–672.

Received: May 28, 2008
Published online: August 27, 2008

